J Mater Sci: Mater Electron (2011) 22:217–222
DOI 10.1007/s10854-010-0116-9

Thermomigration and electromigration in Sn8Zn3Bi solder joints

X. Gu · K. C. Yung · Y. C. Chan · D. Yang

Received: 19 January 2010 / Accepted: 5 April 2010 / Published online: 18 April 2010
© Springer Science+Business Media, LLC 2010

Abstract Individual effect of thermomigration (TM) and combined effect of TM and electromigration (EM) on the microstructural variation in Sn8Zn3Bi was investigated by stressing line-type Au/Ni–P/Cu-Sn8Zn3Bi-Au/Ni–P/Ni solder joints with a 5×10^3 A/cm^2 alternating current (AC) or direct current (DC) at 110°C. Due to the different thermoelectric characteristics of Cu and Ni wires, a thermal gradient of 196°C/cm could be established across the solder joints according to the finite element simulation. In AC current stressing, there is no EM effect and only TM dominates the migration. Microstructural study shows that Zn atoms migrate towards the lower temperature side during TM. In DC current stressing, it is found that both EM and TM play important roles depending various experimental conditions. And the energy change during the EM and the TM is estimated to be $\Delta\omega_{em}$ 3.2×10^{-28} Joule and $\Delta\omega_{em}$ 2.2×10^{-28} Joule, respectively. Upon different current directions in DC current stressing, there is a counteractive or accelerated effect between TM and EM on Zn migration, resulting different microstructures at the cathode side in the solder joints.

X. Gu
Shennan Circuits Co. Ltd., Shenzhen, People's Republic of China

X. Gu · Y. C. Chan (✉) · D. Yang
Department of Electronic Engineering, City University of Hong Kong, Tat Chee Avenue, Kowloon Tong, Hong Kong, People's Republic of China
e-mail: eeycchan@cityu.edu.hk

K. C. Yung
Department of Industrial and Systems Engineering, The Hong Kong Polytechnic University, Hung Hom, Kowloon, Hong Kong, People's Republic of China

1 Introduction

With an increasing awareness of Pb toxicity to environment and human being, Pb-free solders are being widely used in the electronic industry to replace traditional Pb-based solders. Sn8Zn3Bi solder has a low melting point of 197°C, which has encouraged some electronic manufacturers for massive application [1]. Electromigration (EM) in solder joints has become a critical reliability issue for microelectronic device due to continuous miniaturization and demanding requirement of electrical and thermal performance on the interconnect [2]. Recently, thermomigration (TM) has been identified as new reliability concern in solder joints where EM and TM always occurs concurrently [3]. Consequently, there are a few studies on the TM in Pb-free solders [4–10]. However, so far there has been little work published pertaining to the TM behavior in Sn8Zn3Bi solder. Therefore, this study intends to investigate the TM in Sn8Zn3Bi solder using a specific line-type Au/Ni–P/Cu-Sn8Zn3Bi-Au/Ni–P/Ni solder joint.

Generally, it is quite difficult to create and maintain a sufficient thermal gradient across a solder joint to provide sufficient driving force for TM. In a typical flip chip module, there is more Joule heating in the metal trace at the chip side than that that at the substrate side so that a large thermal gradient can be established inside when the heat dissipation is poor [3]. Hsiao and Chen [11] created a thermal gradient of 2,829°C/cm by stressing the Sn3.5Ag FC solder joints with a 1.01×10^4 A/cm^2 alternative constant (AC) current. AC current eliminates the EM effect and facilitates the study of TM. In this study, we applied a new structure made of two fine metal lines and one solder ball, Au/Ni–P/Cu-Sn8Zn3Bi-Au/Ni–P/Ni, for TM characterization under AC or direct current (DC) stressing. Since Cu and Ni have a different thermoelectric behavior, a

thermal gradient is expected to be built in the line-structure solder joint.

2 Experimental

A line-type structure was designed by joining one Cu wire, one Sn8Zn3Bi solder ball and one Ni wire, all with a diameter of 300 μm, using reflow processes. First, the wire end was polished to be flat with a 0.05 μm Al_2O_3 suspension. Then, the end was plated by an electroless Ni–P coating and an immersion Au layer, 2 μm and 0.15 μm, respectively, in thickness. These Au/Ni–P layer were applied as they have been widely used as a surface metallization in electronic packaging. Next, a flux coated solder ball was placed in between the ends of wires, which were aligned inside a glass capillary with an inner diameter of 320 μm. Finally, the assembly was fixed inside the capillary and then soldered in a forced convection reflow oven (BTU PYRAMAX 100N). The peak in soldering profile was 230°C and the time above the melting point of eutectic Sn8Zn3Bi was about 88 s. After solidification, a line-type Au/Ni–P/Cu-Sn8Zn3Bi/Au/Ni–P/Ni solder joint was formed and the capillary glass tube was removed. The width of the solder bump between the two wire ends is in a range of 250–280 μm.

The samples were adhered to a V-groove on a flame retardant 4 (FR4) substrate and aged in a furnace set at 110°C. A constant current of 3.3 A (5×10^3 A/cm^2) was applied to stress solder joints. Both AC (frequency 50 Hz) and DC currents were applied for different testing groups. The AC is particularly for EM elimination since current changes direction frequently. The local temperatures at the solder joint surface were monitored by a thermocouple attached to it during the test. The maximum temperature difference between the two wires was about 67°C and the Cu wire side had a lower temperature due to its small resistance and large thermal conductivity. After different periods of time, the samples were powered off and then cross sectioned carefully towards the center of solder joint. Metallurgical analysis was performed using a Philips XL 40 FEG scanning electron microscope (SEM) equipped with an energy dispersive x-ray spectroscopy (EDX) system.

3 Results and discussion

Figure 1 shows typical microstructure of the solder-to-Ni–P interface in an as-reflowed solder joint. It is well known that in the reaction of Au/Ni–P with Sn–Pb or Sn-Ag solders, Au dissolves into the bulk solder quickly, and then Ni_3Sn_4 intermetallic compound (IMC) formed at the interface. However, the interfacial reaction between Au/Ni–P and Sn8Zn3Bi solder was found to be different as that shown in Fig. 1, Au-Zn IMC formed at the interface due to a fast reaction of Au with Zn. There is no obvious Ni–Zn or Ni–Sn IMC formed at the interface or in the bulk solder. The EDX results showed the chemical composition of Au-Zn layer to be 19.2 at% Au and 80.8 at% Zn. According to the results reported by Yoon et al. [12], it is $AuZn_3$ IMC, instead of Ni-Zn or Ni–Sn IMC, that was formed as a typical IMC layer in a SnZnBi-Au/Ni–P reaction system during reflow.

Figure 2 shows the microstructures of two solder joints stressed with 5×10^3 A/cm^2 AC current at 110°C after different periods of time. Figure 2a–c are the images for one solder joint being stressed after 144 h, and Fig. 2d–f for another solder joint after 384 h.

In the solder joint after the AC current stressing for 144 h, some small Zn-rich phases were created at the solder-to-Au/Ni–P/Cu interface, as shown in Fig. 2b. By contrast, a Sn-rich area with few Zn phases embedded formed at the interface of the Ni side, as shown in Fig. 2c. An IMC layer formed at the solder-to-Au/Ni–P/Ni interface, and EDX analysis shows that about 7.3 at% Ni are contained in this Sn-rich area. According to Yoon et al. it can be regarded as $(Au,Ni)Zn_3$ IMC [12]. The formation of $(Au,Ni)Zn_3$ phase is due to the diffusion of Ni to solder matrix (or the $AuZn_3$ IMC layer) during long-term aging at high temperature. A ternary IMC generally has a lower

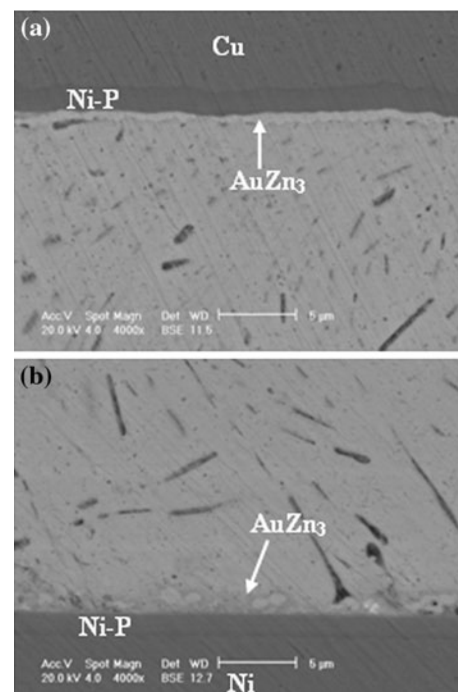

Fig. 1 SEM images of the solder-to-Au/Ni–P interface in an as-reflowed sample: **a** Au/Ni–P/Cu side, **b** Au/Ni–P/Ni side

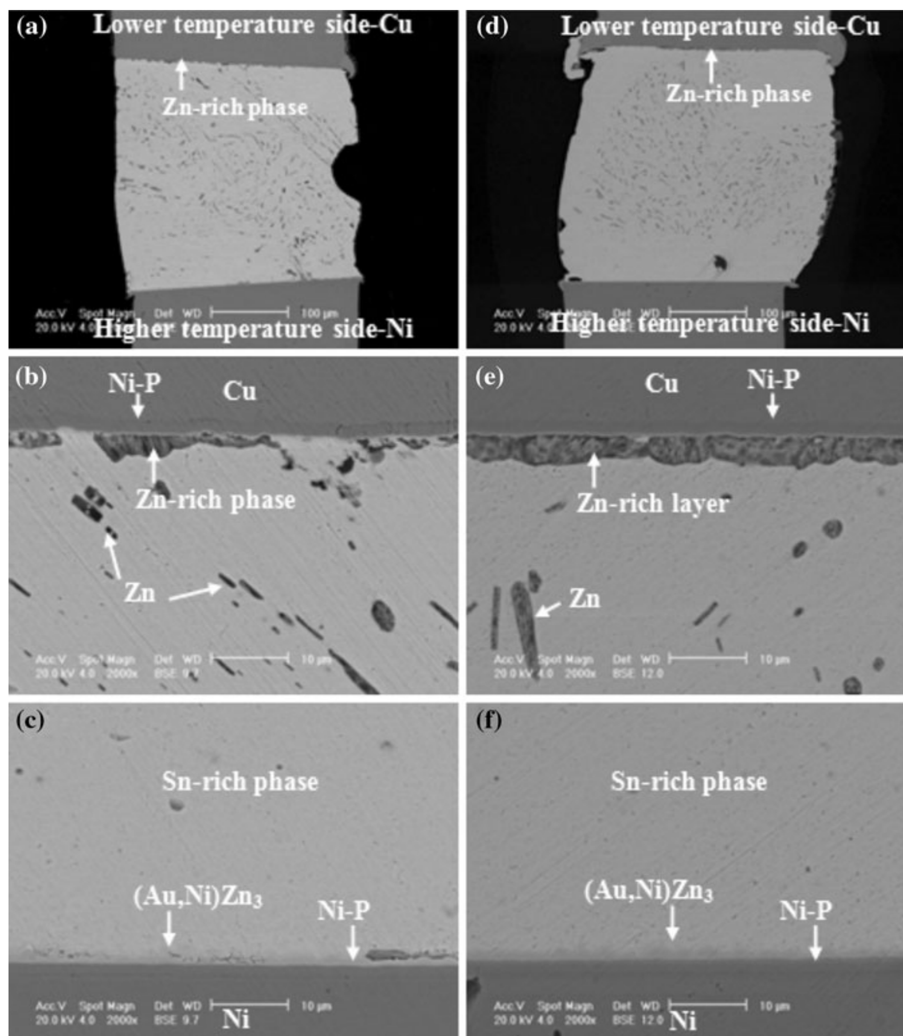

Fig. 2 SEM images of line-type solder joints being stressed with a 5×10^3 A/cm^2 AC current at 110°C: **a** After 144 h, **b** Au/Ni–P/Cu side after 144 h, **c** Au/Ni–P/Ni side after 144 h, **d** After 384 h, **e** Au/Ni–P/Cu side after 384 h, **f** Au/Ni–P/Ni side after 384 h

Gibbs free energy than a binary compound of the same structure from an entropy argument.

In the solder joint after the AC current stressing for 384 h, a 5.2 μm thick layer of Zn-rich area was accumulated at the solder-to-Au/Ni–P/Cu interface, as shown in Fig. 2e. However, at the Au/Ni–P/Ni side the growth of (Au,Ni)Zn_3 IMC layer was insignificant. Meanwhile, it is noted that Ni constitute of the IMC increases to be about 14.1 at%, as compared with that at the solder-to-Au/Ni–P/Cu interface. This suggests that the diffusion of Ni to solder with current stressing.

One important message from above microstructural images is that Zn atoms migrate from the Au/Ni–P/Ni side towards the Au/Ni–P/Cu side. According to the measurement of local temperatures, it is clear that the Au/Ni–P/Cu side is the lower temperature end. Therefore, there is a thermal gradient established from the Au/Ni–P/Ni side toward the Au/Ni–P/Cu side. It is assumed there is no EM effect in the solder joint under an AC current stressing due to the high frequency [11], the atomic migration observed is attributed to the TM driven by thermal gradient. Then, we can conclude that Zn atoms migrate towards the lower temperature end when the solder joint is undergoing a thermal gradient.

For the interfaces of Cu side of the two solder joints shown in Fig. 2, the Au-Zn IMC layers were very thin and this can be ascribed to the dissolution of the Au-Zn IMC into the Zn-rich phase. It is worth noting that no obvious Ni-Zn IMC formed at both interfaces of the solder joint even stressed for 384 h, which indicated that the growth rate of Ni-Zn IMC is very slow and hence Ni-Zn reaction is minor.

For comparison, the microstructural characteristic of line-type Au/Ni–P/Cu-Sn8Zn3Bi-Au/Ni–P/Ni solder joints after DC current stressing was also studied. Figure 3 shows SEM images of two Au/Ni–P/Cu-Sn8Zn3Bi-Au/Ni–P/Ni solder joints being stressed with a 5×10^3 A/cm^2 DC current at 110°C for 384 h. Figure 3a–c are the images for one solder joint with a current flow direction from

Au/Ni–P/Cu (cathode) to Au/Ni–P/Ni(anode), and Fig. 3d–f for the opposite direction in another solder joint. The current flow directions are described by arrows in Fig. 3a, d.

According to Fig. 3b, a Zn-rich layer of 1.7 μm formed at the Au//Ni–P/Ni anode side, which is composed of 90.6 at% Zn, 4.5 at% Au and 4.9 at% Sn. This is a Zn-rich phase rather than an IMC phase. As compared with Fig. 1a, most of $AuZn_3$ IMC layer was disappeared due to dissolution of $AuZn_3$ into Zn-rich phase. It is easy to understand the dissolution of the $AuZn_3$ IMC in the Zn-rich phase as the fast reaction rate between the Zn and Au. Therefore, a very thin and discontinuous $AuZn_3$ IMC can be observed. At the Au/Ni–P/Cu cathode side as shown in Fig. 3c, $AuZn_3$ layer is continuous. Comparing with Fig. 2c, we can find that the $AuZn_3$ IMC layer remains stable at this side after current stressing. In addition, some voids formed between solder and $AuZn_3$ IMC.

In Fig. 3e, it is obvious that a large amount of Zn atoms migrate to the Au//Ni–P/Cu anode side. Some gray particles are also visible in the Zn-rich layer, which are confirmed to be $AuZn_3$ IMC particles. In Fig. 3f of Au/Ni–P/Ni cathode side, thicker Sn-rich layer is formed as compared with that in Fig. 3c. However, their morphology is similar. Nevertheless, no obvious Ni-Zn IMC can be observed in solder joints, regardless of the current flow direction.

It is noted that in DC current stressing, the $AuZn_3$ remains stable at the cathode side (Fig. 3c), which is different from that at the Au/Ni–P/Ni side in AC current (Fig. 2c). This difference can be ascribed to the diffusion of Ni into the solder during DC current stressing. For the solder joint in DC current stressing, the electric current causes $(Au,Ni)Zn_3$ dissolution and then Ni atoms are released. Therefore, no Ni atoms can be detected in the $AuZn_3$ IMC.

Since the current distribution in powered solder joints is independent on the current direction or polarity, Joule heating rate is the same for both the DC and AC cases. Then, the same magnitude of DC current was applied to

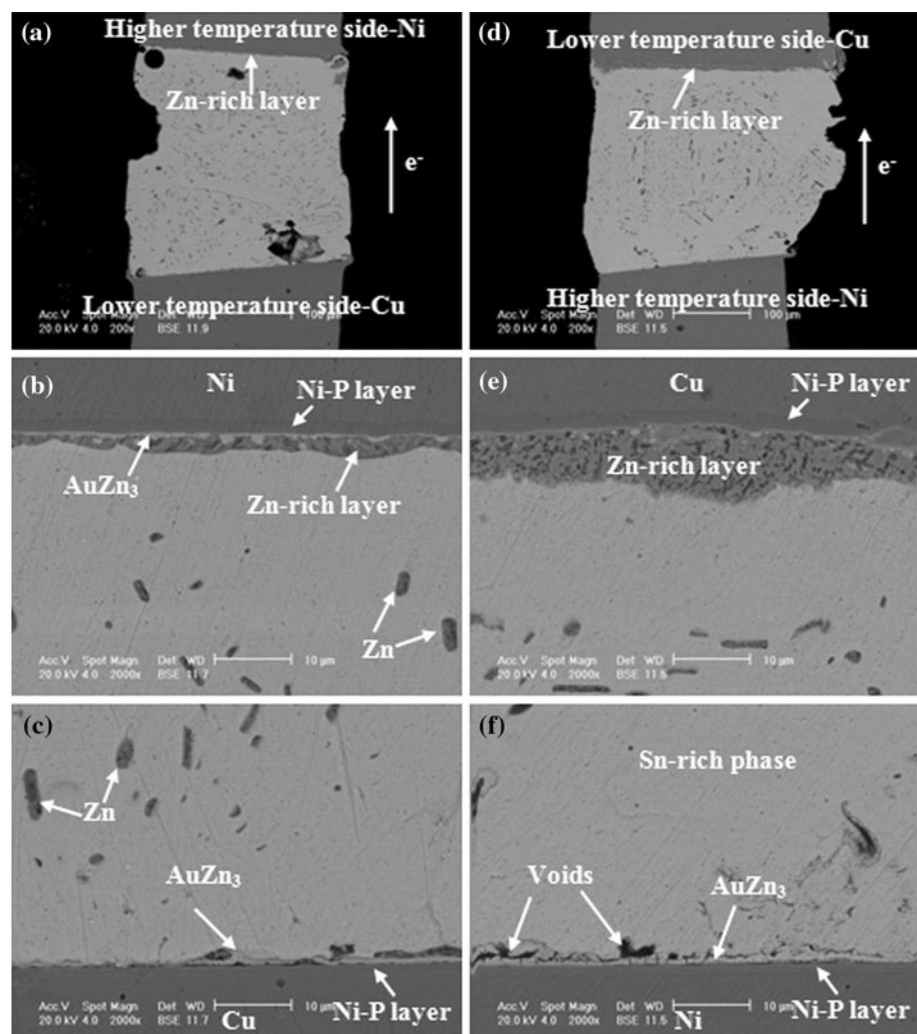

Fig. 3 SEM images of two Au/Ni–P/Cu-Sn8Zn3Bi-Au/Ni–P/Ni solder joints being stressed with a 5×10^3 A/cm^2 DC current at 110°C for 384 h: **a** Current from Au/Ni–P/Cu to Au/Ni–P/Ni, **b** Au/Ni–P/Ni anode, **c** Au/Ni–P/Cu cathode, **d** Current from Au/Ni–P/Ni to Au/Ni–P/Cu, **e** Au/Ni–P/Cu anode, **f** Au/Ni–P/Ni cathode

simulate the temperature distribution in the solder joint stressed with AC current. A three-dimensional coupled electric thermal finite element (FE) modelling was conducted to simulate the temperature distribution in the test structure. In the simulation model, the width of solder bump between two wire ends is set as 260 μm. The physical parameters are tabulated in Table 1 [13–15]. TCR represents temperature coefficient of resistance. The result is shown in Fig. 4.

Figure 4a shows the simulation result of the temperature distribution in a Au/Ni–P/Cu-Sn8Zn3Bi-Au/Ni–P/Ni solder joint stressed with a 5 × 10^3 A/cm^2 DC current at 110°C. The maximum temperature difference between the two wires is above 77.2°C. Figure 4b shows the temperature distribution in the solder bump only. It is clear that a temperature difference of about 5.1°C exists across 260 μm in the solder. The corresponding thermal gradient across the solder is 196°C/cm. This thermal gradient is lower than the simulated value on Cu/Sn58Bi/Ni solder joints in our previous study [10]. This is reasonable since Sn8Zn3Bi has a higher thermal conductivity than Sn58Bi.

Table 1 Properties of materials used in simulation

Material	Thermal conductivity (W/m°C)	Resistivity (μΩ cm)	TCR (10^{-3}/°C)
Cu	398	1.7	4.3
Ni	90.5	7.8	6.8
Ni–P	9.32	70	6.8
Sn8Zn3Bi	61	15	4.6

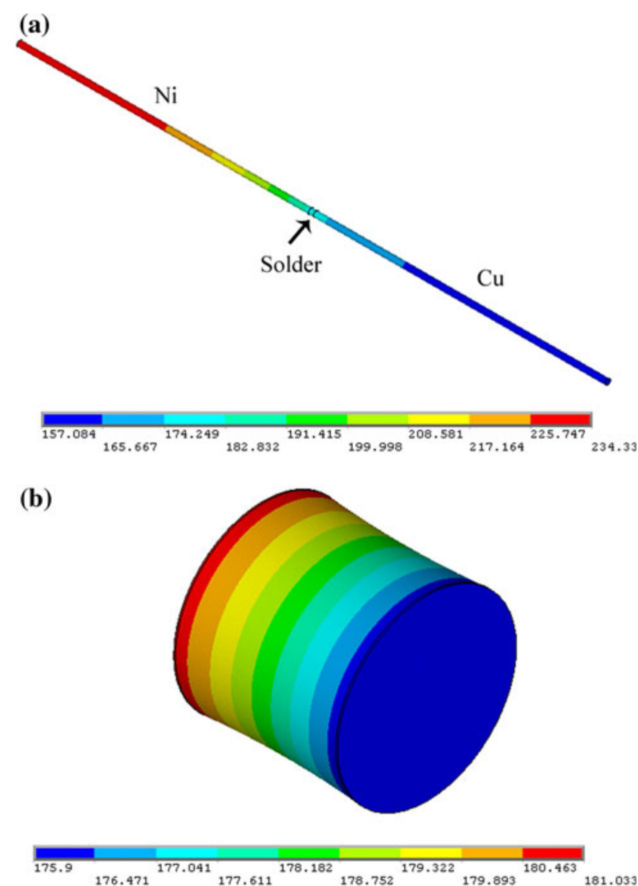

Fig. 4 Temperature distribution in the line-type Au/Ni–P/Cu-Sn8Zn3Bi-Au/Ni–P/Ni structure with a 5 × 10^3 A/cm^2 current stressing at 110°C: **a** overall distribution, **b** distribution in the solder bump (units: °C)

According to the results reported by Ouyang et al. [16], the thermal energy change by driving force of TM can be expressed as:

$$\Delta\omega_{tm} = 3k\Delta T = 3\,kdg \quad (1)$$

where d is the atomic diameter, g is the thermal gradient and k is Boltzmann's constant. The energy change by driving force of EM can be expressed as:

$$\Delta\omega_{em} = Z^{*}e\rho jd \quad (2)$$

where $Z*$ is the effective charge number of metal atom, e is the electron charge, j is the current density, ρ is the resistivity and d is the atom diameter.

Taking the atom diameter of Zn (2.78 × 10^{-8} cm) and thermal gradient (g) into Eq. (1), the thermal energy change by driving force of TM can be obtained. Also, taking the effective charge number Z^* of Zn in Sn (2.5) [17], the current density (5 × 10^3 A/cm^2), resistivity of Zn (5.9 × 10^{-6} Ω cm) and the atom diameter (2.68 × 10^{-8} cm) into Eq. (2), the thermal energy change by the driving force of EM can be obtained. $\Delta\omega_{em}$ is calculated to be 3.28 × 10^{-28} Joule, and $\Delta\omega_{em}$ is 2.26 × 10^{-28} Joule. Since both energy variations are comparable, the Zn atomic flux induced by TM in the solder cannot be ignored during current stressing study by DC. Then, we can conclude that in the Au/Ni–P/Cu-Sn8Zn3Bi-Au/Ni–P/Ni solder joint under a 5 × 10^3 A/cm^2 DC current at 110°C, both TM and EM could induce the migration of Zn atoms.

According to the results in the AC current case, Zn atoms migrate towards the lower temperature side when the solder joint undergoes TM. It is known that the Zn atomic flux which induced by EM is in the same direction as the electron flow. For the joint stressed with the current flow from the Au/Ni–P/Cu (cathode side) to the Au/Ni–P/Ni (anode side), the Zn atomic flux induced by EM is in an opposite direction to that induced by TM. Then, the effect of TM counteracts with the effect of EM on Zn diffusion. By contrast, for the joint stressed with the current flow from the Au/Ni–P/Ni (cathode side) to the Au/Ni–P/Cu (anode side), the Zn atomic flux induced by EM is in the same direction as that induced by. Then, the effect of TM assists the effect of EM on Zn diffusion. Therefore, Zn migration will be in an accelerated manner.

It is rational that the Zn-rich layer formed by accelerated migration shown in Fig. 3e is much thicker than that by retardant migration in Fig. 3b.

4 Conclusions

In conclusion, the TM behavior of Sn8Zn3Bi solder was investigated by stressing the line-type Au/Ni–P/Cu-Sn8Zn3Bi-Au/Ni–P/Ni solder joints with AC current. A thermal gradient with magnitude of 196°C/cm was created across the solder joint with a 5×10^3 A/cm^2 AC or DC current at 110°C.

In the AC current stressing study, only TM occurred without the effect of electric current. Zn atoms migrate towards the lower temperature side, the Au/Ni–P/Cu end, and Zn-rich phase is formed there. In the DC current stressing study, both EM and TM occurred with an energy change of $\Delta\omega_{em}$ 3.28×10^{-28} Joule and $\Delta\omega_{em}$ 2.26×10^{-28} Joule, respectively. Since they are comparable, there is a counteractive or accelerated effect between TM and EM on Zn migration depending on current direction, resulting different microstructures in the solder joint under DC current stressing.

Acknowledgments The work described in this paper is fully supported by a grant from General Research Fund (GRF) of Hong Kong (Project No. 9041486).

References

1. K. Suganuma, K.S. Kim, J. Mater. Sci.: Mater. Electron. **18**, 121 (2007)
2. K.N. Tu, J. Appl. Phys. **94**, 5451 (2003)
3. H. Ye, C. Basaran, D.C. Hopkins, Appl. Phys. Lett. **82**, 1045 (2003)
4. K.-L. Lin, S.-M. Kuo, in *Proceedings of 56th Electronic Components and Technology Conference,* IEEE, San Diego, CA, 2006, p. 668
5. H.-Y. Hsiao, C. Chen, Appl. Phys. Lett. **94**, 092107 (2009)
6. H.Y. Chen, C. Chen, K.N. Tu, Appl. Phys. Lett. **93**, 122103 (2008)
7. C. Basaran, S. Li, M.F. Abdulhamid, J. Appl. Phys. **103**, 123520 (2008)
8. S. Li, C. Basaran, Mech. Mater. **41**, 271 (2009)
9. M.F. Abdulhamid, C. Basaran, J. Electron. Pack. **131**, 011002 (2009)
10. X. Gu, Y.C. Chan, J. Appl. Phys. **105**, 093537 (2009)
11. H.-Y. Hsiao, C. Chen, Appl. Phys. Lett. **94**, 092107 (2009)
12. J.-W. Yoon, S.-B. Jung, Solder joint reliability evaluation of Sn–Zn/Au/Ni/Cu ball-grid-array package during aging. Mater. Sci. Eng. A **46**, 452–453 (2007)
13. K.J. Puttlitz, K.A. Stalter, *Handbook of Lead-Free Solder Technology for Microelectronic Assemblies* (Marcel Dekker, Inc., New York, 2004), p. 282
14. D.R. Frear, S.N. Burchett, H.S. Morgan, J.H. Lau, *The Mechanics of Solder Alloy Interconnects* (Van Nostrand Reinhold, New York, 1994), p. 61
15. S.W. Liang, Y.W. Chang, C. Chen, J. Electron. Mater. **36**, 159 (2007)
16. F.Y. Ouyang, K.N. Tu, Y.-S. Lai, A.M. Gusak, Appl Phys Lett **89**, 221906 (2006)
17. H.B. Huntington, *Diffusion in Solids: Recent Developments* (Academic Press, New York, 1975), p. 303